

Preparation And Antibacterial Effects Of Carboxymethyl Chitosan-Modified Photo-Responsive *Camellia* Sapogenin Derivative Cationic Liposomes

This article was published in the following Dove Press journal:
International Journal of Nanomedicine

Jin Zhang
Chuan-Zhen Ye
Ze-Yu Liu
Qian Yang
Yong Ye

Department of Pharmaceutical Engineering, School of Chemistry and Chemical Engineering, South China University of Technology, Guangzhou 510640, People's Republic of China

Background: Bacterial resistance to antibiotics is a persistent and intractable problem. The sapogenin isolated from the seeds of *Camellia oleifera* can inhibit antibiotic-resistant bacteria after structural modification.

Purpose: This study aims to improve sapogenin's antibacterial activity and avoid bacterial resistance based on nano-preparation with photo responsiveness.

Methods: The liposome shell material of carboxymethyl chitosan-phosphatidyl ethanolamine (CMC-PE) was prepared using amidation reaction, and photo-responsive cationic (PCC) liposomes containing *Camellia* sapogenin derivative (CSD) and photosensitizer pheophorbide-a were prepared by film dispersion method. Encapsulation efficiency, drug loading, zeta potential, particle size distribution, morphology and stability of the PCC liposomes were determined by HPLC, particle size analyzer, transmission electron microscopy (TEM) and fluorescence microscopy. Photo-responsive release of CSD in the PCC liposomes was determined by laser (0.5 mW/cm²) at 665 nm. Antibacterial activity of the PCC liposomes with or without irradiation was analyzed by MIC₅₀, MBC, MBIC₅₀, and bacterial morphology to evaluate the antibacterial effects on amoxicillin resistant *Escherichia coli* and *Staphylococcus aureus*.

Results: Size distribution, zeta potential, encapsulation efficiency and drug loading of the PCC liposomes were 189.23 ± 2.12 nm, 18.80 ± 1.57 mV, 83.52 ± 1.53% and 2.83 ± 0.05%, respectively. The PCC liposomes had higher storage stability and gastrointestinal stability, and no obvious hemolytic toxicity to rabbit red blood cells and no cytotoxicity after incubation with Hela cells. The photosensitizer pheophorbide-a was uniformly dispersed in the phospholipid layer of the PCC liposomes and increased the CSD release after irradiation. The PCC liposomes could bind to bacteria and impaired their morphology and structure, and had significant bactericidal effect on amoxicillin resistant *E. coli* and *S. aureus*.

Conclusion: The photo-responsive PCC liposomes are efficient antibacterial agents for avoidance of bacterial resistance against antibiotics.

Keywords: *Camellia* sapogenin derivative, photo-responsive cationic liposomes, carboxymethyl chitosan, antibacterial effects, antibiotic substitutes

Correspondence: Yong Ye
Department of Pharmaceutical Engineering, School of Chemistry and Chemical Engineering, South China University of Technology, Guangzhou 510640, People's Republic of China
Tel +86-20-87110234
Email yeyong@scut.edu.cn

Introduction

Antibiotics play important roles in the therapy of pathogenic microorganism infection for a long time.¹ However, the long-term abuse of antibiotics has led to an increase of drug-resistant bacteria, causes great threats to humans and animals, and

poses serious challenges in clinical treatment.^{2,3} The bio-film formation is a crucial factor for the bacteria with antibiotic resistance, the effect of which can escape the destruction from antibiotics and immunocyte through wrapping in their own secreted extracellular polymeric substances.^{4,5} Therefore, it is meaningful to develop alternative new antibacterial agents with multiple antibacterial pathways to avoid resistance. The natural products possess plenty of active compounds with antibacterial activity, which may be exploit as an antibiotic substitute with a lower propensity of bacterial resistance.^{6,7}

Literature indicate that the saponin extracted from *Camellia oleifera* shells has the potential as antibiotic substitutes because of its abundant and cheap resource and low bacterial resistance against antibiotics.^{8,9} Antibacterial effect of the *Camellia* saponin is due to its structure easily binding to the cholesterol of the cell membrane receptor, causing destruction of cell membrane structure and function, and promoting cell lysis.^{9,10} Based on the structure–function relationship, saponin is the main active part of *Camellia* saponin, and could be modified with C₂₈ ester substitutions in favor of dramatically enhancing the antimicrobial activity especially by the introduction of the aromatic ring, heterocyclic ring and strong electron-withdrawing groups.^{11,12}

Liposomes are commonly used drug delivery systems with the advantages of biocompatibility and efficient encapsulation of both hydrosoluble and liposoluble drug.^{13,14} The cationic liposomes have specific antibacterial mechanism and antimicrobial activity through disrupting the integrity of bacterial membrane and wall by electrostatic interaction.^{15–17} This specific mechanism will effectively reduce the risks to develop the bacterial resistance because bacteria can hardly survive from the physical destruction of cellular structure.¹⁸

Carboxymethyl chitosan (CMC) possesses the virtues of similar characters including biodegradability, biocompatibility, bacteriostatic, fungistatic, and better solubility than chitosan.¹⁹ The surface modification of liposomes with CMC could significantly improve the stability of liposomes in vitro and in vivo because of a tight water covering layer formation from the hydration of CMC in the aqueous solution.^{20,21}

Through the increase of drug bioavailability and targeting, the intelligent Nano-drug delivery systems play unique roles in enhancing antibacterial activity and reducing the bacterial resistance.^{22,23} Generally, the liposomes could be physically or chemically modified to be pH responsive,²⁴ thermal responsive,²⁵ magnetic responsive²⁶ and photo responsive²⁷ in order to control drug release. On the basis of our previous finding that photo-responsive liposomes can be prepared by

phospholipid mixed with the pheophorbide-a, a photosensitizer extracted from silkworm excrement, the liposomes had photo responsiveness to red light with no side effects.²⁸ Meantime, the singlet oxygen from photosensitization of pheophorbide-a also had the synergistic antibacterial effect.^{5,29} Therefore, we designed a new kind of CMC-modified photo-responsive *Camellia* saponin derivative cationic liposomes (PCC liposomes) with complex structure shown in Figure 1. Antibacterial activities and biosecurity of the PCC liposomes were, respectively, evaluated, and antibacterial mechanism was analyzed by the integrity of bacterial cell structure.

Materials And Methods

Drugs And Reagents

Camellia saponin derivative (CSD) was obtained from our previous research,³⁰ its synthetic route is shown in Figure 2. Pheophorbide-a was extracted from silkworm feces in our laboratory. N-hydroxysuccinimide (NHS), 1-(3-Dimethylaminopropyl)-3-ethylcarbodiimide hydrochloride (EDC), phosphatidyl ethanolamine (PE), carboxymethyl chitosan (CMC) and maleic anhydride (MAH) were purchased from Macklin Reagent (Shanghai, People's Republic of China). Soybean phosphatidylcholine (SPC) and cholesterol were purchased from Yuanju Biotech (Shanghai, People's Republic of China). Cetrimonium bromide (CTAB), amoxicillin and triton were purchased from Aladdin Reagent (Shanghai, People's Republic of China). Macroporous adsorbent resin (AB-8) was bought from Tianjin Chemical Reagent Factory (Tianjin, People's Republic of China). Phosphotungstic acid dye, spurr resin, uranyl acetate and copper mesh were purchased from Beijing Zhongjingkeyi Technology (Beijing, People's Republic of China). Methyl thiazolyl tetrazolium (MTT) was purchased from Sangon Biotech (Shanghai, People's Republic of China). Mueller-Hinton (MH) broth media, and agar used for bacteria culture were purchased from Hope Biotech (Qingdao, People's Republic of China). SYTOX GREEN dye was bought from Nanjing Kebai Biotech (Nanjing, People's Republic of China). HeLa cells and DMEM medium were obtained from Shanghai Cell Bank (Shanghai, People's Republic of China). Rabbit red blood cells (rRBC) were purchased from Guangzhou Hongquan Biotech (Guangzhou, People's Republic of China).

Bacterial Strains And Culture

The standard strains of *Escherichia coli* (*E. coli*, CMCC44825) and *Staphylococcus aureus* (*S. aureus*, ATCC29213) were purchased from Guangdong Microbiology Culture Center

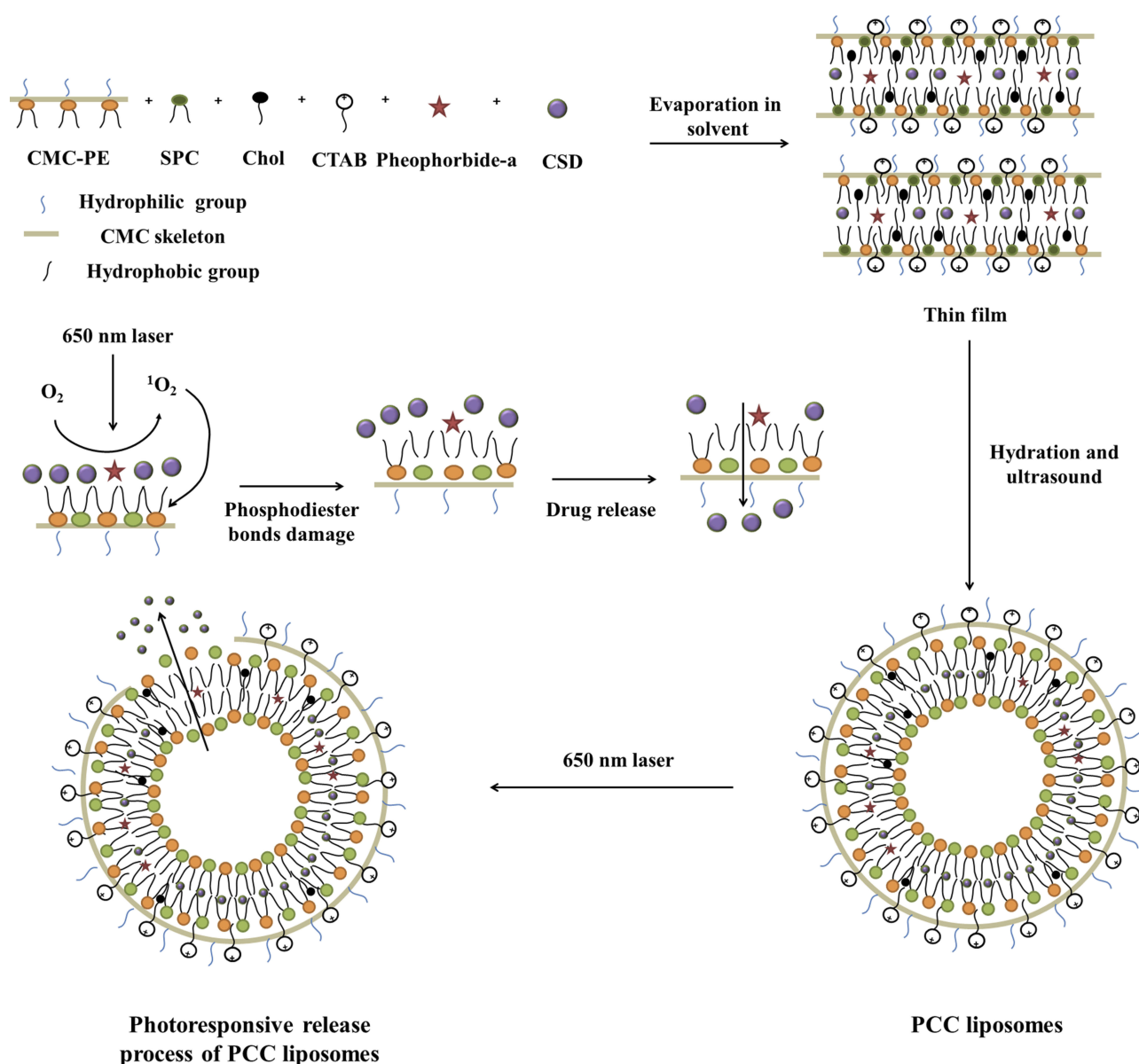


Figure 1 Structure and drug release mechanism of the PCC liposomes.

Abbreviations: PCC, photo-responsive *Camellia* sapogenin derivative cationic; SPC, soybean phosphatidylcholine; Chol, cholesterol; CMC, carboxymethyl chitosan; SPE, phosphatidyl ethanolamine; CTAB, cetrimonium bromide; CSD, *Camellia* sapogenin derivative.

(Guangzhou, People's Republic of China). All bacterial strains were activated, and further cultured at 37°C and shaking of 100 rpm to the exponential growth stage in Mueller-Hinton broth (MH broth). Drug-resistant *E. coli* and *S. aureus* strains were induced by amoxicillin according to the reference.³¹

Synthesis Of PE-MAH

CMC-PE as a new shell material of nanocapsule was synthesized by amidation reaction of PE, MAH and CMC, the scheme is illustrated in Figure 3. The PE-MAH and CMC-PE were synthesized step by step

according to our previously described procedure with some modification.³⁰ To a PE (1.0 g) in CHCl₃ (20 mL), MAH (0.15 g) was added at room temperature, and then the triethylamine (100 μL) was added to the reaction solution. The mixture was reacted at 55°C for 12 h. After the completion of the reaction, the solvent was removed by rotary evaporation, and the residue was washed with acetone (10 mL×3), lyophilized to obtain PE-MAH (0.94 g). The structure of the obtained PE-MAH was determined by FTIR (Bruker Company, Karlsruhe, Germany), ¹H-NMR (Bruker Company, Karlsruhe, Germany), elemental

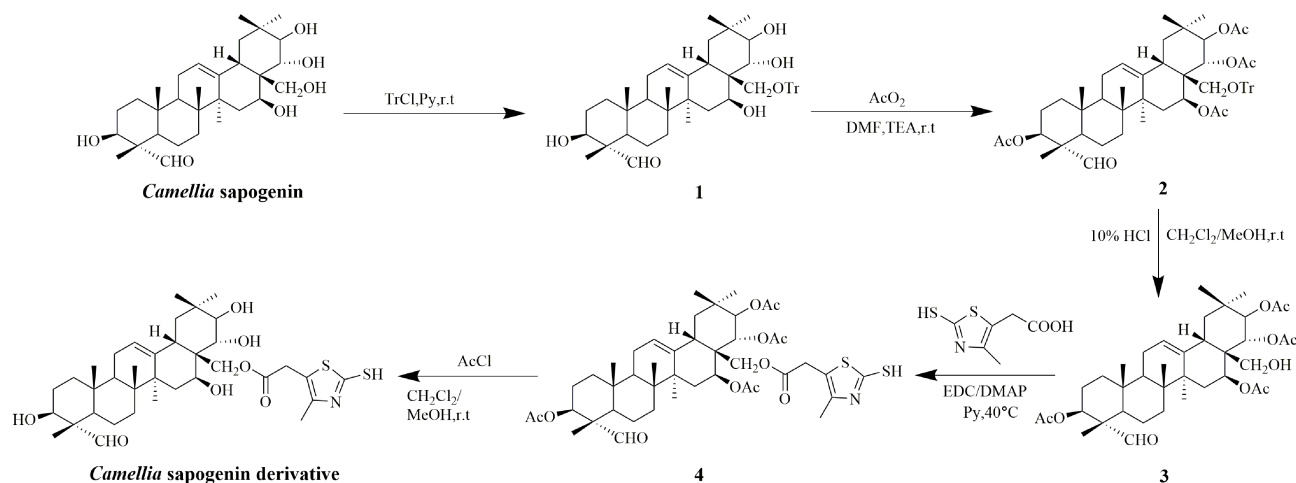


Figure 2 Synthetic route of *Camellia sapogenin* derivative.

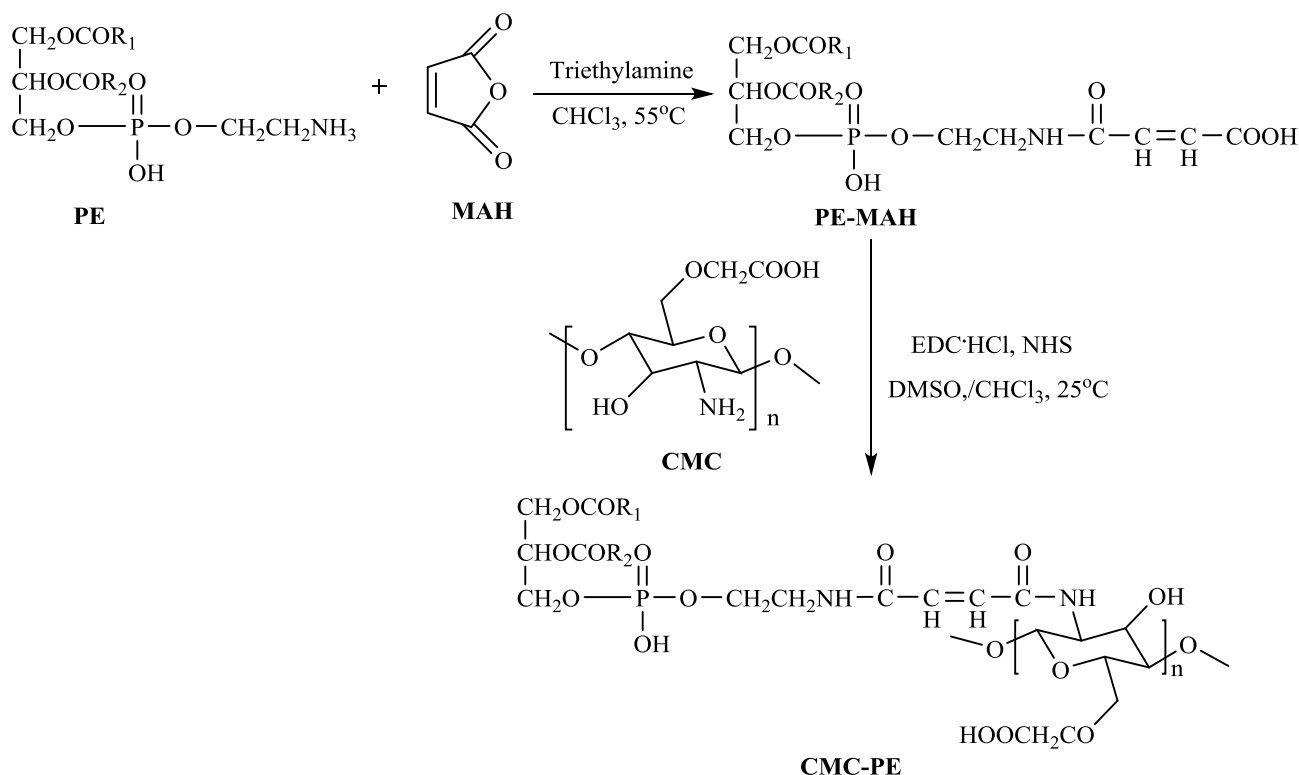


Figure 3 Synthetic route of PE-MAH and CMC-PE.

Abbreviations: CMC, carboxymethyl chitosan; MAH, maleic anhydride; PE, phosphatidyl ethanolamine.

analysis (Saberhagen Company, Zurich, Switzerland) and stored at 4°C for further application.

Synthesis Of CMC-PE

EDC HCl (0.27 g) and NHS (0.16 g) were added to a solution of PE-MAH (1.0 g) in DMSO/CHCl₃ (v: v, 2: 1) at room temperature. After stirring for 2 hrs, a solution of CMC (0.05 g, 5 mL) in DMSO/deionized water (v: v, 2: 1) was added

dropwise at room temperature. Reaction mixture was further stirred for 72 hrs at the same temperature. After the completion of the reaction, the resulting solution was dialyzed in a dialysis bag (14,000 Da molecular weight cutoff) to remove unreacted reagent and small molecular species, and subsequently lyophilized to obtain CMC-PE (0.76 g). The structure of the obtained CMC-PE was determined by FTIR, ¹H-NMR, elemental analysis, and stored at 4°C for further application.

Preparation Of Photo-Responsive CSD Cationic Liposomes

A lipid film hydration method was applied to prepare drug-loaded cationic liposomes.³² Briefly, CSD (60 mg), CMC-PE (420 mg), SPC (420 mg), cholesterol (85 mg), pheophorbide-a (10 mg) were dissolved in chloroform (10 mL), and the thin lipid film was formed by rotary evaporation at 50°C for 30 mins and further dried under vacuum at 35°C. Then, it was hydrated at 40°C by adding 5 mL of 6% CTAB phosphoric acid solution (pH=7.4) and sonicated for 5 mins. Finally, the PCC liposomes were obtained by passing through 0.22 µm pore diameter polycarbonate filters and stored at 4°C until use. Preparation of control liposomes using the same method, including normal blank liposomes (without CTAB, CSD and pheophorbide-a), blank cationic liposomes (without CSD and pheophorbide-a), photosensitive blank liposomes (without CSD), and contrast liposomes (without CMC-PE).

Determination Of Encapsulation Efficiency And Drug Loading

Encapsulation efficiency (EE) and drug loading (DL) of the PCC liposomes were determined by mini-column centrifugation-HPLC.³³ The liposomes (0.5 mL) were added in macroporous resin microcolumn (AB-8, 3 mL) and centrifuged at 4000 rpm for 1 min to remove unencapsulated CSD, and then extracted with 10 mL of methanol, sonicated for 5 mins to destroy the liposomes and passed through a 0.22 µm filter. The filtrate was determined by HPLC to get the content of encapsulated CSD (W_i). The analysis of CSD was run on HP 1100 HPLC (Agilent Company, California, USA) in the following operating conditions: column: Hypersil ODS (250 × 4.6 mm, 5 µm); flow phase: methanol/water (90/10); injection volume: 20 µL; flow rate: 1.0 mL/min; temperature: 30°C; wavelength: 250 nm. Another 0.5 mL of liposomes solution were extracted with 10 mL of methanol, and ultrasonically demulsified, and the total drug content (W_t) was determined under the same HPLC conditions.

EE and DL of the PCC liposomes were calculated according to the following equations:

$$EE(\%) = \frac{W_i}{W_t} \times 100\% \quad (1)$$

$$DL(\%) = \frac{W_i}{W} \times 100\% \quad (2)$$

where W_i is the amount of drug in the liposomes, W_t is the total drug content, and W is the weight of liposomes containing drug.

Measurement Of Liposomes Size Distribution And Zeta Potential

Size distribution (PSD) and zeta potential of the liposomes were measured in this research using a Nano-2S MDT-2 Malvern particle size analyzer (Malvern Instruments Limited, Malvern, UK). The liposomes (1mL) were dispersed in 10 mL of deionized water and then measured at 25°C with the refractive index 1.33. Data were calculated as the average of 3 repetitions.

Morphological Observation Of Liposomes

Morphology of the PCC liposomes was observed by transmission electron microscopy (TEM) and inverted fluorescence microscope (FM). The PCC liposomes were diluted to a concentration of 0.5 µg/mL with deionized water, and dropped on to a glass slide and observed by IX83 inverted fluorescence microscope (Japan Olympus Co., Ltd., Tokyo, Japan) under white light and purple light (Excitation wavelength: 395–415 nm). Morphology of the PCC liposomes was further observed under TEM (JEOL, Tokyo, Japan) with the following treatment. The liposomes were stained for 2 mins with a staining agent (2% phosphotungstic acid), dropped onto a copper grid, and dried in air for 6 hrs at room temperature before observation.

Stability Test Of Liposomes

Physical stability of the liposomes was evaluated by the change of particle size, zeta potential and encapsulation efficiency after storage at 4°C for 8 weeks. Biostability of the PCC liposomes was evaluated by the acid tolerance of simulated gastric fluid (SGF, 1% pepsin, pH=1.2) and the digestive tract enzyme degradation of simulated intestinal fluid (SIF, 1% trypsin, pH=6.8).³³ Briefly, the PCC liposomes (1 mL) were added to SGF or SIF (4 mL) and incubated at 37°C shaking with a rate of 100 rpm. After sampling 0.5 mL at regular intervals, the leachate by microcolumn centrifugation was extracted with 5 mL of methanol, and sonicated for 5 mins. The CSD concentration in the filtrate was determined by HPLC. The percentage of residual CSD was calculated to evaluate the stability of the liposomes.

Drug Release Test Of PCC Liposomes

UV-Vis absorption spectra and fluorescence spectra of the PCC liposomes were measured at 200–800 nm using an ultraviolet spectrophotometer (Shimadzu, co., Ltd., Tokyo, Japan) and a fluorescence spectrofluorometer (Shimadzu,

co., Ltd., Tokyo, Japan) respectively. The liposomes were irradiated at 665 nm red light (0.5 mW/cm^2) for 0, 10, 20, 40, 60 mins. Then, the liposomes (2 mL) were added into 23 mL of PBS (0.1 M, pH=7.4) solution and incubated at 37°C shaking with a rate of 100 rpm. At predetermined time intervals (0.5, 1.0, 2.0, 4.0, 8.0, 10.0, 12.0, 24.0 hrs), the solution (200 μL) was taken and diluted with methanol to 1 mL, sonicated for 5 mins. The content of CSD released was determined by HPLC, and the mean release percentages were calculated.

Bacterial Growth Inhibition And Biofilm Inhibition Assay

Antibacterial activity of the PCC liposomes against *S. aureus* and *E. coli* was determined using the standard broth micro-dilution method.⁹ The bacteria were diluted to 5×10^5 CFU/mL by MH broth. The PCC liposomes were dissolved in DMSO to make 100 mg/mL solution, and diluted by MH broth to make the series of final concentration at 256, 128, 64, 32, 16, 8, 4, 2, 1 and 0.5 $\mu\text{g/mL}$. Dilutions of the PCC liposomes (100 μL) were sequentially added into the 96-well plates, which were inoculated with tested bacteria (100 μL), and incubated at 37°C for 24 hrs. The OD value at wavelength of 600 nm (OD_{600}) was measured by CYTATION5 micro-plate spectrometer (BioTeck Company, America) and bacterial growth inhibition rate was calculated as follows. The minimum inhibitory concentration on 50% bacterial strains was calculated as MIC_{50} . The wells treated without amoxicillin, CSD and the liposomes were used as negative treatments.

$$\text{Bacterial growth inhibition rate (\%)} = \frac{(\text{Negative OD}_{600} - \text{Drug OD}_{600})}{\text{Negative OD}_{600}} \times 100\% \quad (3)$$

The negative control suspension (50 μL) was evenly spread on Muller Hinton agar and cultivated at 37°C for 24 hrs. Bacterial colonies in the plates were counted to calculate the number of bacteria in the corresponding wells. Minimum bactericidal concentration (MBC) indicates the minimum concentration of drug required to kill more than 99.99% of the tested strains according to the CLSI standard.³⁴

Bacterial biofilm experiments were carried out by crystal violet staining.^{35,36} After culture medium in 96-well plates were removed and washed 3 times with PBS (0.1 M, pH=7.4), 0.1% crystal violet solution (100 μL) was added in each well to dye the biofilm. Fifteen minutes later, the solution was aspirated. All wells were washed 3 times with

PBS (0.1 M, pH=7.4), and then 33% glacial acetic acid solution (100 μL) was added to extract crystal violet from the biofilm. The absorbance at 570 nm (OD_{570}) was measured to calculate the biofilm inhibition rate. The minimum bacterial biofilm inhibitory concentration on 50% bacterial strains was calculated as MBIC_{50} .

$$\text{Biofilm inhibition rate (\%)} = \frac{\text{Negative OD}_{570} - \text{Drug OD}_{570}}{\text{Negative OD}_{570}} \times 100\% \quad (4)$$

The antibacterial activity of CSD, normal blank liposomes, blank cationic liposomes and photosensitive blank cationic liposomes was tested by the above method.

Hemolysis Assay

The liposomes were determined for their hemolytic rate against rabbit red blood cell (rRBC).³⁷ Fresh rRBC were washed thrice with saline by centrifugation at 3000 rpm for 5 mins and were suspended in saline. The liposomes (1 mL) were then added to 1 mL of rRBC solution. The mixture suspension was incubated at 37°C for 1 hr. The rRBC morphology was observed under inverted fluorescent microscope, the suspension was then centrifuged at 3000 rpm for 5 mins. Finally, the absorbance of the supernatant was measured at 540 nm. The positive control was 1% triton, and the negative control was saline. The percentage of hemolysis was defined as

$$\text{Hemolysis rate (\%)} = \frac{\text{Drug OD}_{540} - \text{Negative OD}_{540}}{\text{Positive OD}_{540} - \text{Negative OD}_{540}} \quad (5)$$

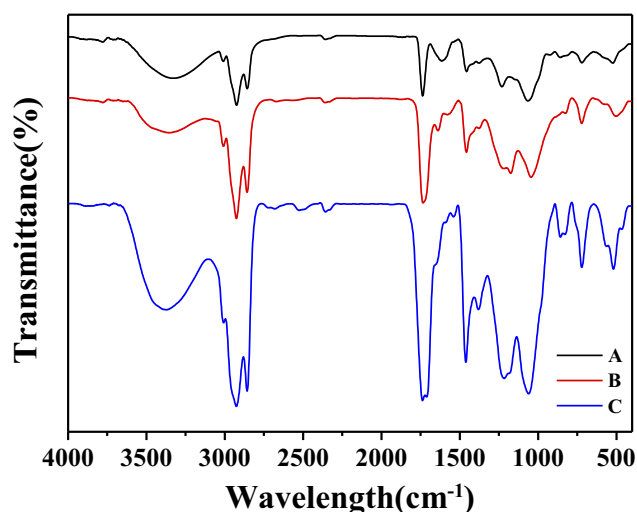


Figure 4 FTIR spectra of PE (A), PE-MAH (B) and CMC-PE (C). **Abbreviations:** CMC, carboxymethyl chitosan; MAH, maleic anhydride; PE, phosphatidyl ethanolamine.

Morphological Observation Of Bacteria

The morphology of both *S. aureus* and *E. coli* was examined with scanning electron microscopy (SEM) and TEM. *S. aureus* and *E. coli* were incubated with 2×MIC the PCC liposomes under the same conditions as the bactericidal

test, respectively. MH broth was used as a blank control, and normal blank liposomes were used as a negative control. To prepare SEM samples, the untreated and treated bacteria were centrifuged to remove the supernatant, and the remaining precipitate was fixed with 2.5% glutaraldehyde for 12 hrs

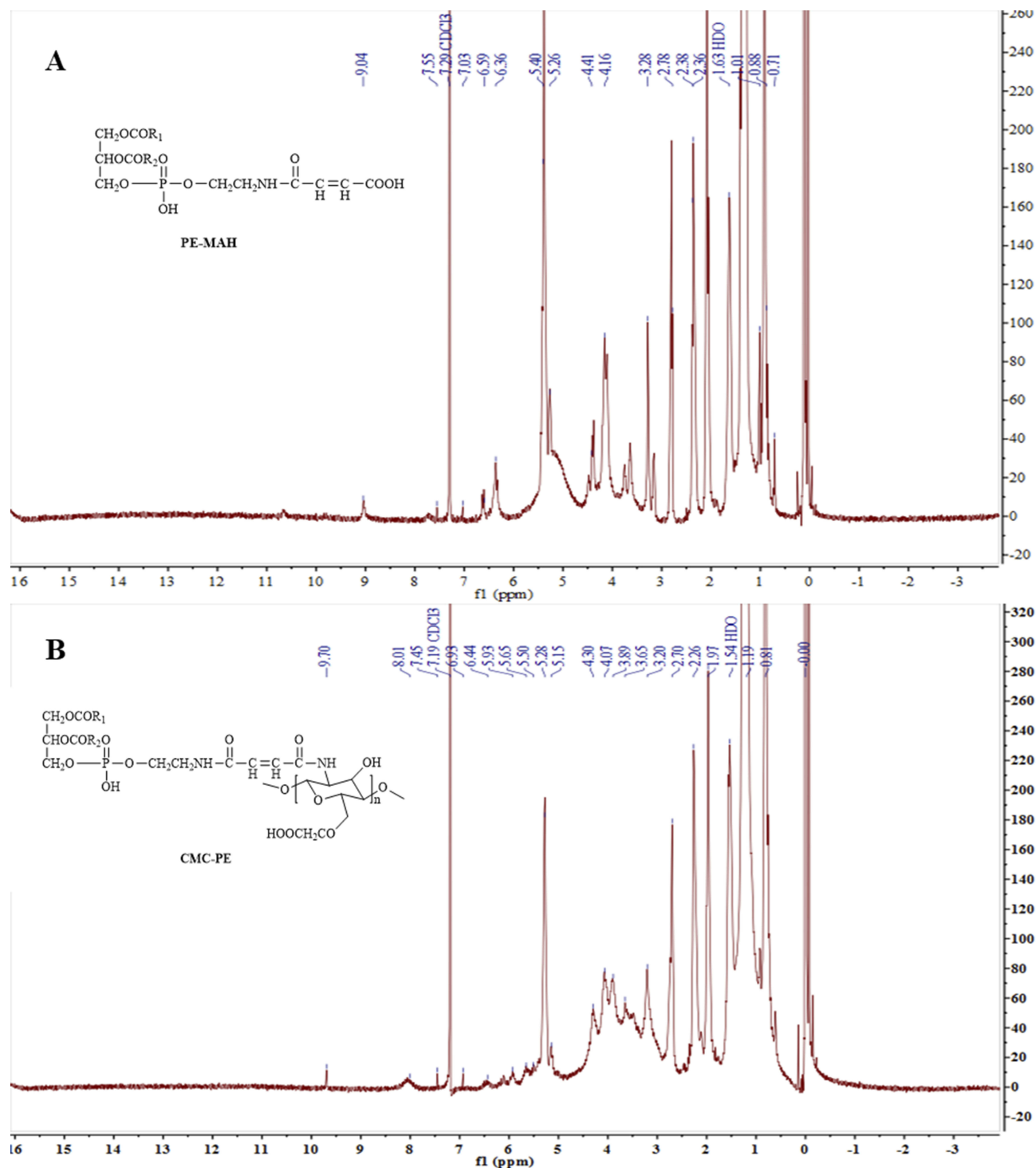


Figure 5 $^1\text{H-NMR}$ spectra of PE-MAH (A) and CMC-PE (B).

Abbreviations: CMC, carboxymethyl chitosan; MAH, maleic anhydride; PE, phosphatidyl ethanolamine.

at 4°C. After fixation, the samples were centrifuged to remove glutaraldehyde and resuspended in 50 μL of t-butanol. Then, the bacterial suspension (3 μL) was dropped on the mica slides, lyophilized and coated with gold before SEM imaging. For TEM observation, bacteria were fixed with 2.5% glutaraldehyde and 1% osmium tetroxide and

embedded in spurr resin, and then stained with uranyl acetate before TEM imaging.

Cell Culture And Cytotoxicity Assay

The cytotoxicity was evaluated by MTT assay on cell viability.³⁸ HeLa cells were incubated in DMEM medium

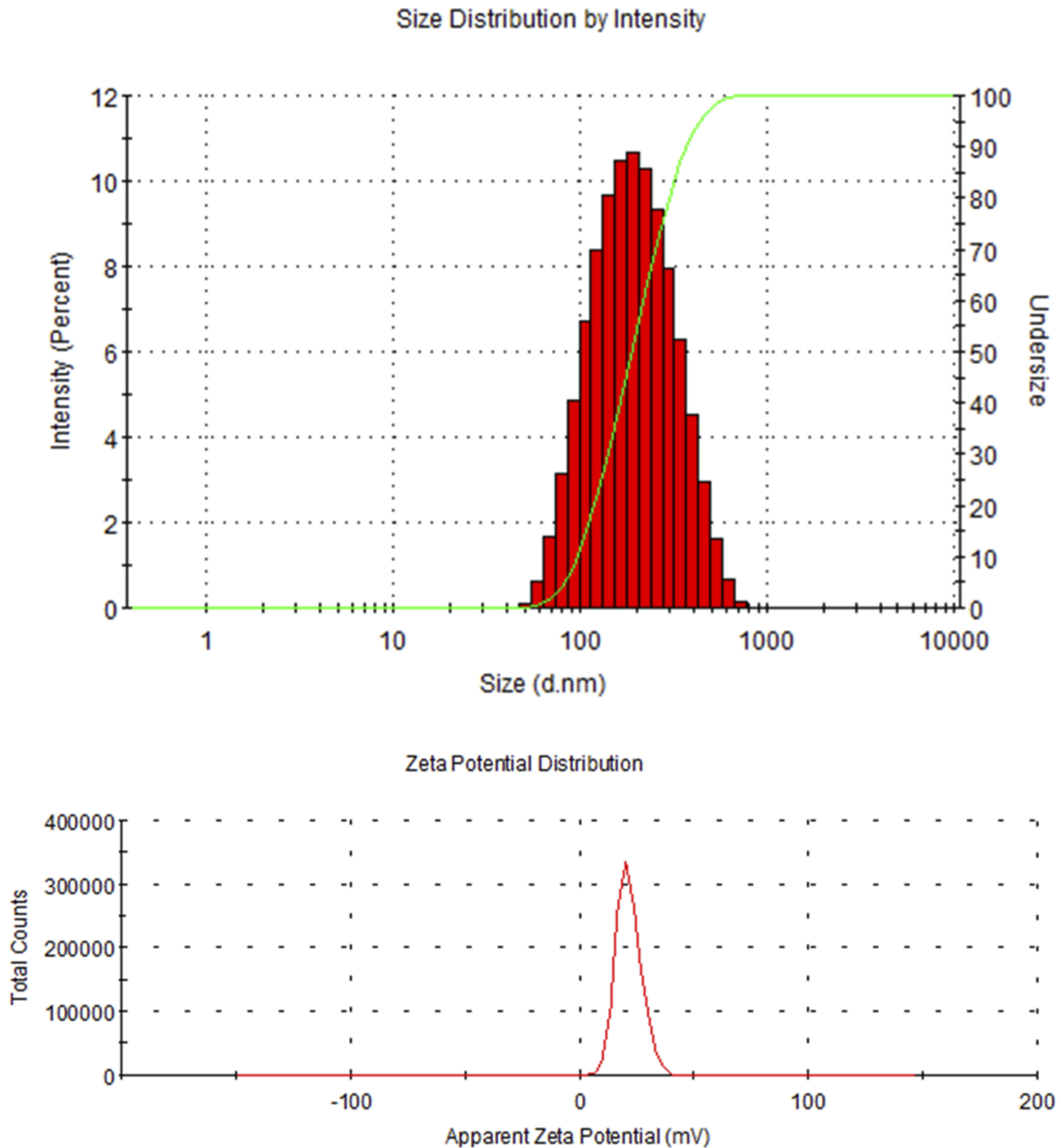


Figure 6 Size distribution and zeta potential of the PCC liposomes.
Abbreviations: PCC, photo-responsive *Camellia* sapogenin derivative cationic.

for 24 hrs in 96-well plates (37°C, 5% CO₂) and divided into the groups of normal liposomes, blank cationic liposomes and the PCC liposomes. The medium was replaced with fresh medium containing different concentrations of liposomes and incubated for an additional 24 hrs. Then, MTT solution (20 μL) was added and incubated at 37°C for 4 h. Finally, the absorbance was measured at 490 nm using DMEM medium as the negative control. The percentage of HeLa cell survival was defined as

$$\text{HeLa cell survival rate (\%)} = \frac{\text{Drug OD}_{490}}{\text{Negative OD}_{490}} \times 100\% \quad (6)$$

Statistical Analysis

All data were expressed as mean ± standard deviation, and analyzed with SPSS17.0 software to obtain statistical results. The significant levels of the treatments in

antibacterial tests, EE and DL, average size and zeta potential, drug release percentage, hemolysis rate and cell survival rate were calculated using one-way ANOVA and Student–Newman–Keuls (SNK) tests.

Results And Discussion

Synthesis And Characterization Of CMC-PE

In order to prepare the PCC liposomes, the hydrophilic carrier material CMC-PE was synthesized by amidation reaction and characterized by FTIR spectroscopy and ¹H-NMR. As shown in Figure 4, the new peaks at 1710 cm⁻¹ and 1550 cm⁻¹ in FTIR spectroscopy demonstrated the formation of amide bonds, indicating the existence of amide groups in CMC-PE. Moreover, CMC-PE presented higher peaks at 3393 cm⁻¹ and 1740 cm⁻¹ than PE-MAH, suggesting that it was successfully connected to the CMC.

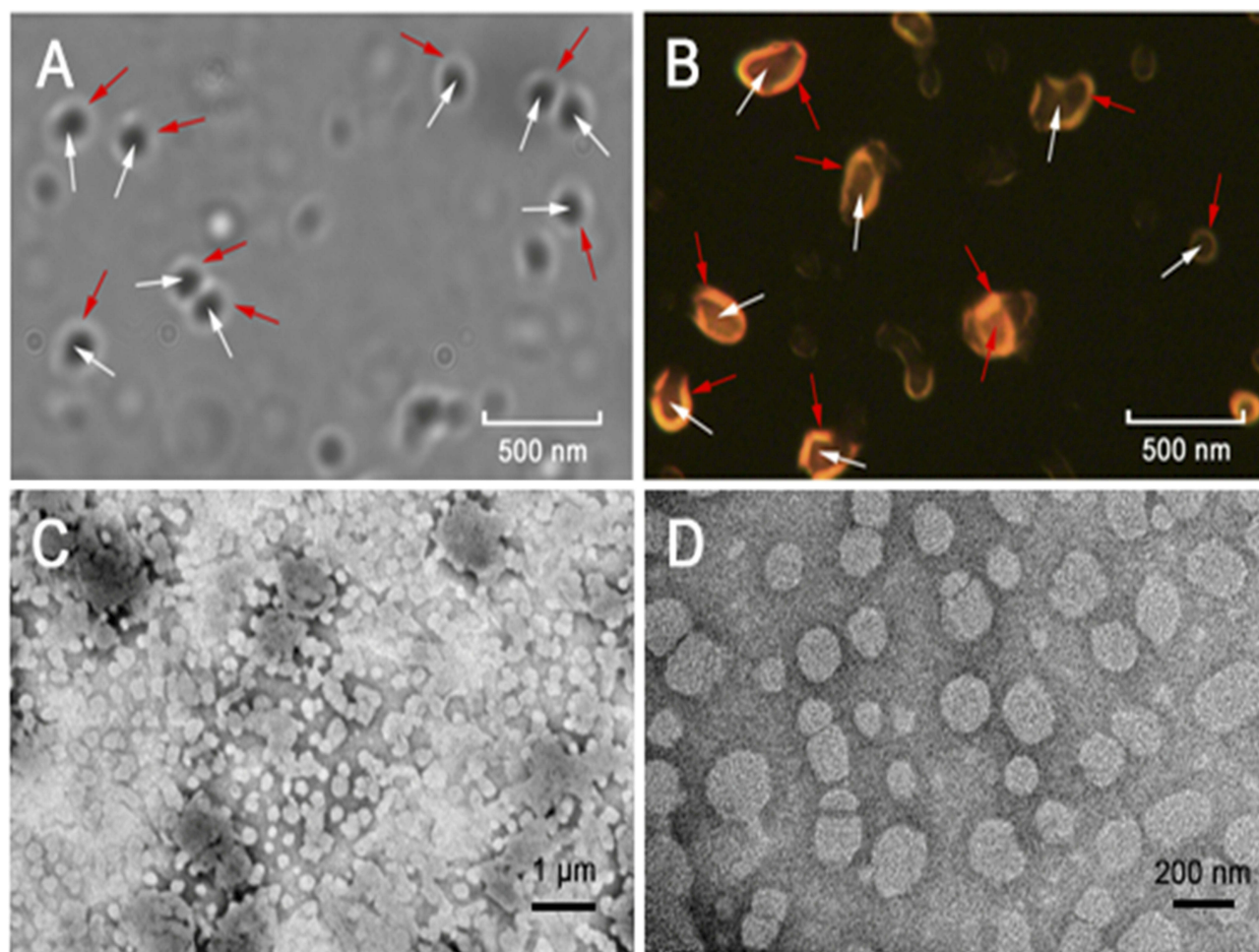


Figure 7 Fluorescence photographs of the PCC liposomes under white light (A) and 415 nm light excitation (B). TEM images of PCC liposomes. Scale bar = 1 μm (C) and 200 nm (D). **Notes:** Red arrows represent pheophorbide-a in the outer shell and white arrows represent *Camellia* sapogenin derivative in the inner core of PCC liposomes. **Abbreviations:** PCC, photo-responsive *Camellia* sapogenin derivative cationic; TEM, transmission electron microscopy.

Correspondingly, the ^1H NMR Spectra of PE-MAH and CMC-PE in Figure 5 showed the new peaks at approximately 9.04 ppm, which is consistent with previously reported spectra of amide groups.¹⁹ In addition, the signals at approximately 4.30 ppm occurred in CMC-PE, which were attributed to the carboxymethyl proton signal peak of carboxymethyl chitosan. The above results indicate that PE-MAH was successfully grafted onto the amino group of CMC. Elemental analysis showed that the graft ratio was 87.89%.

Nanostructure Of The PCC Liposomes

The PCC liposomes with uniform size distribution were fabricated by thin-film dispersion method. The EE and DL were, respectively, $83.52 \pm 1.53\%$ and $2.83 \pm 0.05\%$. The PCC liposomes had the size of 189.23 ± 2.12 nm and zeta potential of 18.80 ± 1.57 mV (Figure 6), and well dispersed as individual particles with dispersion index (PDI) 0.34. The positive charge is due to the presence of CTAB on the PCC liposomes.³⁹

Morphology of the PCC liposomes was visualized and photographed under TEM and fluorescence microscope. Images of the PCC liposomes revealed good dispersity (Figure 7) and sphericity with red fluorescence in shell layers (Figure 7B). Among the components of the PCC liposomes, only pheophorbide-a had red fluorescence under UV excitation. Thus, it was predominantly distributed within the phospholipid bilayer.

Stability Of The PCC Liposomes

Storage stability of the PCC liposomes at 4°C was examined by encapsulation efficiency, zeta potential and average size, as shown in Figure 8. It showed that particle average size, zeta potential and encapsulation efficiency of the PCC liposomes changed very little after storage over 8 weeks at 4°C . It indicates strong stability in storage. On the other hand, the gastrointestinal tract stability was evaluated by the retention rates of CSD in the liposomes of SGF and SIF. The result is shown in Figure 9. The retention rates of contrast liposomes (without CMC-PE) after incubation for 4 hrs in SGF and SIF were 49.02% and 59.52%, but those of the PCC liposomes in SGF and SIF were 81.74% and 85.92%, respectively, indicating that gastrointestinal stability of the liposomes modified by CMC-PE was significantly improved. The possible mechanism is that CMC could form a dense hydrophilic protective film on the surface of

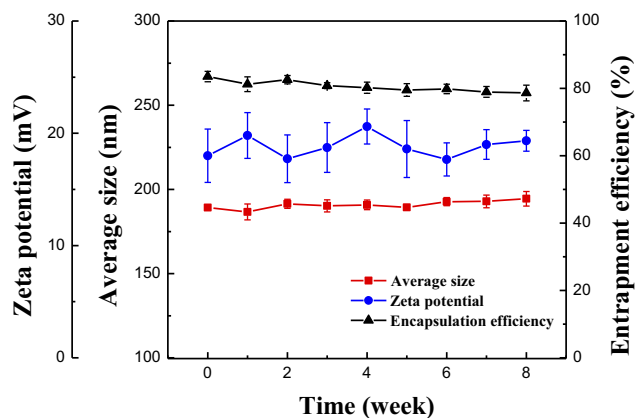


Figure 8 Changes of average size, zeta potential and encapsulation efficiency of the PCC liposomes stored at 4°C for 8 weeks.

Abbreviation: PCC, photo-responsive *Camellia* sapogenin derivative cationic.

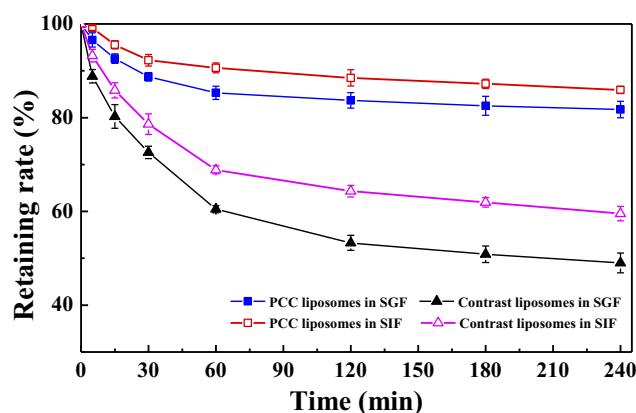


Figure 9 Retention rate of CSD in the PCC liposomes and contrast liposomes (without CMC-PE) in SGF and SIF.

Abbreviations: CSD, *Camellia* sapogenin derivative; PCC, photo-responsive *Camellia* sapogenin derivative cationic; SGF, simulated gastric fluid; SIF, simulated intestinal fluid; CMC, carboxymethyl chitosan; PE, phosphatidyl ethanolamine.

PCC liposomes to reduce the penetration of gastrointestinal fluid into liposomes, and extend the cycle time of drugs encapsulated in liposomes.²¹ Therefore, the PCC liposomes have both physical stability and biostability, and can take effects for a long time.

Photo-Responsive Drug Release Of PCC Liposomes

As shown in Figure 10, the PCC liposomes have UV absorption at 410 nm and 665 nm, which is consistent with the UV absorption characteristic peak of pheophorbide-a, and the fluorescence spectra showed a strong emission peak at 673 nm under 665 nm excitation. It indicates that the pheophorbide-a in the PCC liposomes could be activated under red light (665 nm). Therefore, CSD release from the PCC liposomes was evaluated by the

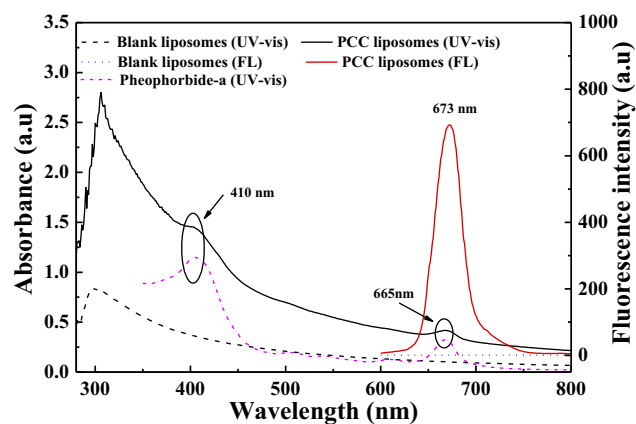


Figure 10 The UV-Vis and FL spectra of the PCC liposomes, normal blank liposomes and pheophorbide-a.

Abbreviations: PCC, photo-responsive *Camellia* sapogenin derivative cationic; UV-Vis, ultraviolet-visible; FL, fluorescence.

accumulative amount caused by pheophorbide-a photosensitive effect under 665 nm irradiation, the result is shown in Figure 11. The PCC liposomes were irradiated for 10, 20, 40, 60 mins, and the cumulative release rate at 12 hrs reached 62.94%, 74.53%, 89.28% and 92.20%, respectively. However, the maximum CSD release from the PCC liposomes without irradiation only reached 21.62% within 12 hrs. It indicates that the PCC liposomes have photo responsiveness, and 665 nm irradiation dramatically improves CSD release from the liposomes.

Why is drug release efficiency strengthened by pheophorbide-a in the liposomes after irradiation? In photodynamic therapy, the cause of cell death is the local production of singlet oxygen by photosensitizer. The main mechanism of its cytotoxicity is that the singlet oxygen can destroy the phosphodiester bond of the cell

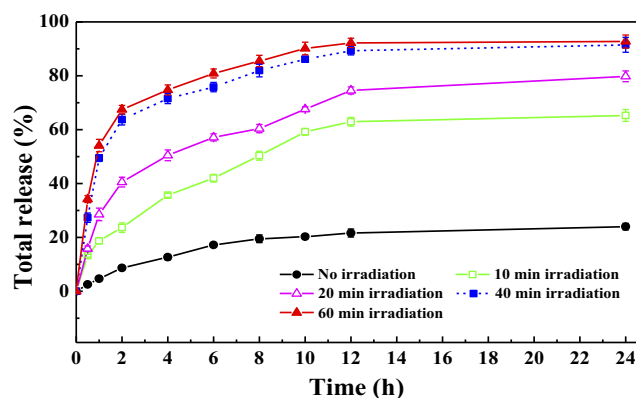


Figure 11 Cumulative release curves of CSD from the PCC liposomes at different illumination times (10, 20, 40, 60 mins).

Abbreviations: PCC, photo-responsive *Camellia* sapogenin derivative cationic; CSD, *Camellia* sapogenin derivative.

membrane and cause cytoplasmic leakage. Pheophorbide-a, an effective photosensitizer, can generate singlet oxygen while excited by 665 nm laser. Therefore, the photoactivated release mechanism of CSD from the PCC liposomes is attributed to destroy of lecithin's phosphodiester bonds of the liposomes by pheophorbide-a produced singlet oxygen.²⁸

Hemolysis And Cytotoxicity Of The Liposomes

Since the cationic surfactant CTAB is a quaternary ammonium salt, easily leads to hemolysis with cytotoxicity,³⁹ the safety of PCC liposomes was preliminarily evaluated by erythrocyte hemolysis. The toxicity of PCC liposomes was measured by the hemolytic potential toward rRBC. As shown in Figure 12, less than 1% rRBC were lysed when incubated with the PCC liposomes (32 $\mu\text{g}/\text{mL}$), whose hemolytic activity was similar to normal blank liposomes, suggesting little hemolytic toxicity of the PCC liposomes. The rRBC morphology is shown in Figure 13A, the 1% triton-treated rRBC became an irregular polygonal shape. However, the rRBC treated with normal blank liposomes (Figure 13B), blank cationic liposomes (Figure 13C) and the PCC liposomes (Figure 13D) have a complete spherical structure with a smooth surface, indicating that the PCC liposomes are safe and almost free of hemolysis toxicity at 32 $\mu\text{g}/\text{mL}$ of concentration.

The cytotoxicity was further investigated by Hela cells cultured with DMEM medium containing different concentrations of the liposomes for 24 hrs, and evaluated by MTT colorimetry. The results are shown in Figure 14.

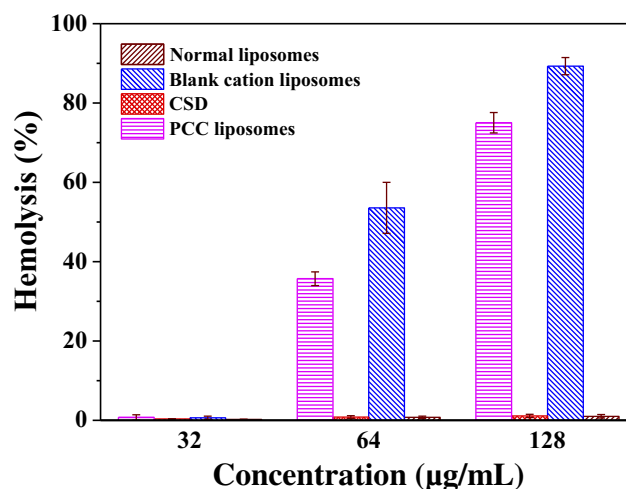


Figure 12 Hemolysis percentage of the PCC liposomes, blank cation liposomes, normal liposomes and CSD.

Abbreviations: PCC, photo-responsive *Camellia* sapogenin derivative cationic; CSD, *Camellia* sapogenin derivative.

When the PCC liposomes concentration was 4.0 $\mu\text{g/mL}$, the cell survival rate was 98.72%. Therefore, no obvious cytotoxicity exists for the PCC liposomes.

Antibacterial Activities Of The PCC Liposomes

MIC₅₀ and MBC of the PCC liposomes against *S. aureus* and *E. coli* were determined by microdilution method, and MBIC₅₀ of bacterial biofilm was determined by crystal violet staining. Amoxicillin was used as a drug-resistant

control, and normal blank liposomes were used as a negative control. Table 1 summarizes the MIC₅₀, MBC and MBIC₅₀ values of CSD, normal blank liposomes, blank cationic liposomes, photosensitive blank liposomes and the PCC liposomes against both *S. aureus* and *E. coli*. The results showed that amoxicillin could not inhibit the growth of *S. aureus* and *E. coli*, and MIC₅₀, MBC and MBIC₅₀ of the PCC liposomes were significantly lower than those of CSD. The results indicate that the bacteria are resistant against amoxicillin, and the PCC liposomes

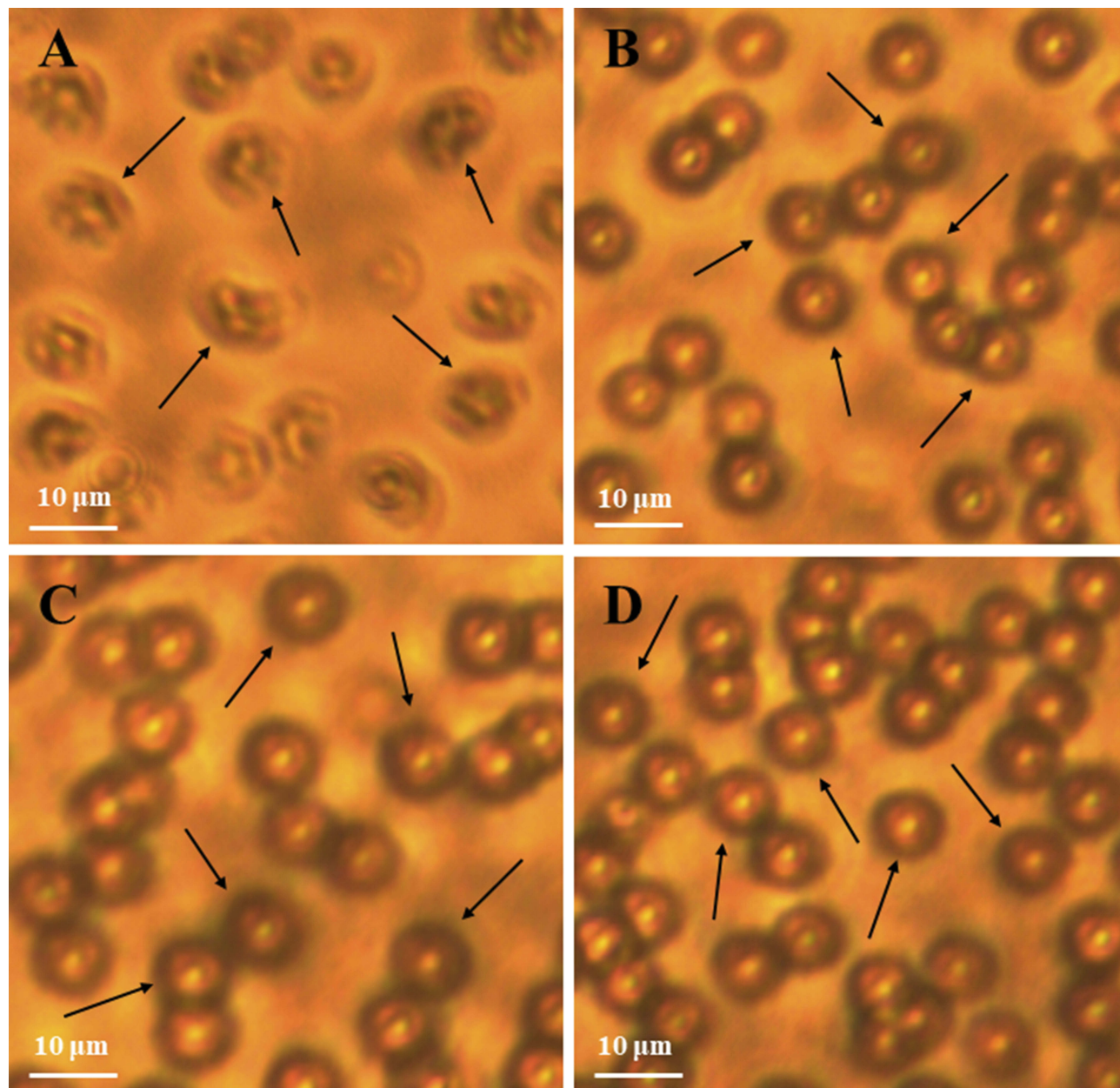


Figure 13 Morphology of rRBC after treatment with 1% triton (A), normal blank liposomes (B), blank cationic liposomes (C) and PCC liposomes (D) observed by inverted fluorescence microscope.

Abbreviations: PCC, photo-responsive *Camellia* saponin derivative cationic; rRBC, rabbit red blood cells.

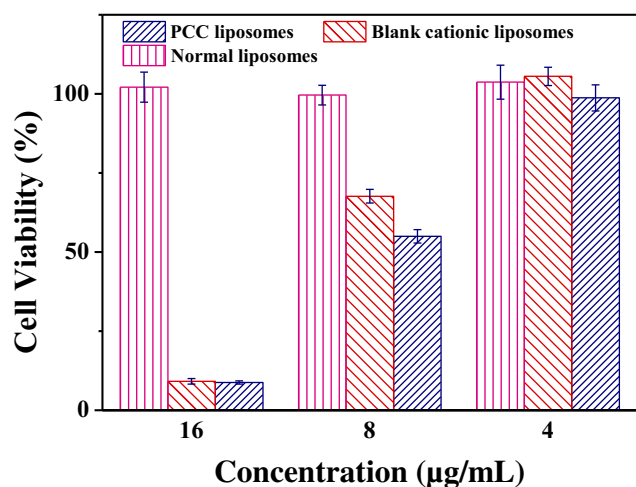


Figure 14 Cytotoxicity of the PCC liposomes, normal blank liposomes, blank cationic liposomes on HeLa cells after 24 hrs of incubation.

Abbreviation: PCC, photo-responsive *Camellia* sapogenin derivative cationic.

significantly increased the antibacterial activity on amoxicillin resistant bacteria.

The morphology transformation of *S. aureus* and *E. coli* was examined using SEM and TEM. The image shows that typical *S. aureus* cells and *E. coli* cells have normal spherical morphology and rod-like morphology, respectively, and both have intact cell membranes (Figure 15A, C, E, G). After bacteria were treated with the PCC liposomes for 2 hrs, microbial cells severely aggregated and completely lost their normal shape. It further confirms that the PCC

liposomes can severely damage bacteria and make bacterial cell lysis (Figure 15B, D, F, H).

Antibacterial activity of the PCC liposomes was significantly higher than that of CSD, blank cationic liposomes and photo-responsive blank liposomes, indicating that the PCC liposomes have synergistic antibacterial effects and can prevent bacterial resistance, the combined action of CSD, pheophorbide-a and cationic liposomes destroys bacterial biofilm structure and function, and accelerates the dissolution and death of the drug-resistant bacteria.

The antibacterial mechanism of the PCC liposomes relies on CSD structure, positive charge and photodynamic effects. CSD is an antibacterial compound, and its nano-capsulation improves the antibacterial effects. Since the positive charge on the surface of the cationic liposomes is easily combined with the negative charge of the bacterial cell membrane phospholipid, it changes the cell membrane permeability and destroys the bacterial cell structure, strengthens antibacterial activity. On the other hand, the photo-responsive liposomes produced significant differences in antibacterial activity under without illumination and illumination conditions, illumination significantly improved the antibacterial activity. It means that the photosensitizer pheophorbide-a has photodynamic effects, and generates singlet oxygen under the excitation of 665

Table I Antibacterial Activity Of The Liposomes (unit: µg/mL)

Groups Without Illumination	<i>S. aureus</i>			<i>E. coli</i>		
	MIC ₅₀	MBC	MBIC ₅₀	MIC ₅₀	MBC	MBIC ₅₀
Amoxicillin	/	/	/	/	/	/
CSD	2.67±0.65	40	2.38±0.09	18.08±1.21	160	17.82±0.12
Normal blank liposomes	/	/	/	/	/	/
Blank cationic liposomes	0.55±0.01	2.0	0.46±0.01	1.94±0.07	4.0	1.70±0.15
Photosensitive blank liposomes	0.57±0.01	2.0	0.45±0.02	1.88±0.03	4.0	1.80±0.05
PCC liposomes	0.19±0.004	2.0	0.22±0.006	1.21±0.04	4.0	0.89±0.08
Groups With 665 nm Illumination	<i>S. aureus</i>			<i>E. coli</i>		
	MIC ₅₀	MBC	MBIC ₅₀	MBIC ₅₀	MBC	MBIC ₅₀
Amoxicillin	/	/	/	/	/	/
CSD	2.52±0.42	40	2.36±0.15	18.63±0.92	160	17.01±0.68
Normal blank liposomes	/	/	/	/	/	/
Blank cationic liposomes	0.54±0.02	2.0	0.46±0.01	2.03±0.12	4.0	1.69±0.15
Photosensitive blank liposomes	0.32±0.02	2.0	0.29±0.01	1.39±0.08	4.0	1.22±0.01
PCC liposomes	0.13±0.002	0.5	0.11±0.002	0.72±0.02	2.0	0.45±0.02

Notes: Data are presented as mean ± standard deviation (n=3). All data show significant differences between treatments ($p < 0.05$). MIC₅₀ indicates the minimum inhibitory concentration of the drug required to inhibit the growth of 50% of the tested strain; MBC indicates the minimum concentration of drug required to kill more than 99.99% of the tested strains; MBIC₅₀ indicates the minimum concentration of drug required to inhibit biofilm formation by 50% of the tested strains.

Abbreviations: PCC, photo-responsive *Camellia* sapogenin derivative cationic; CSD, *Camellia* sapogenin derivative.

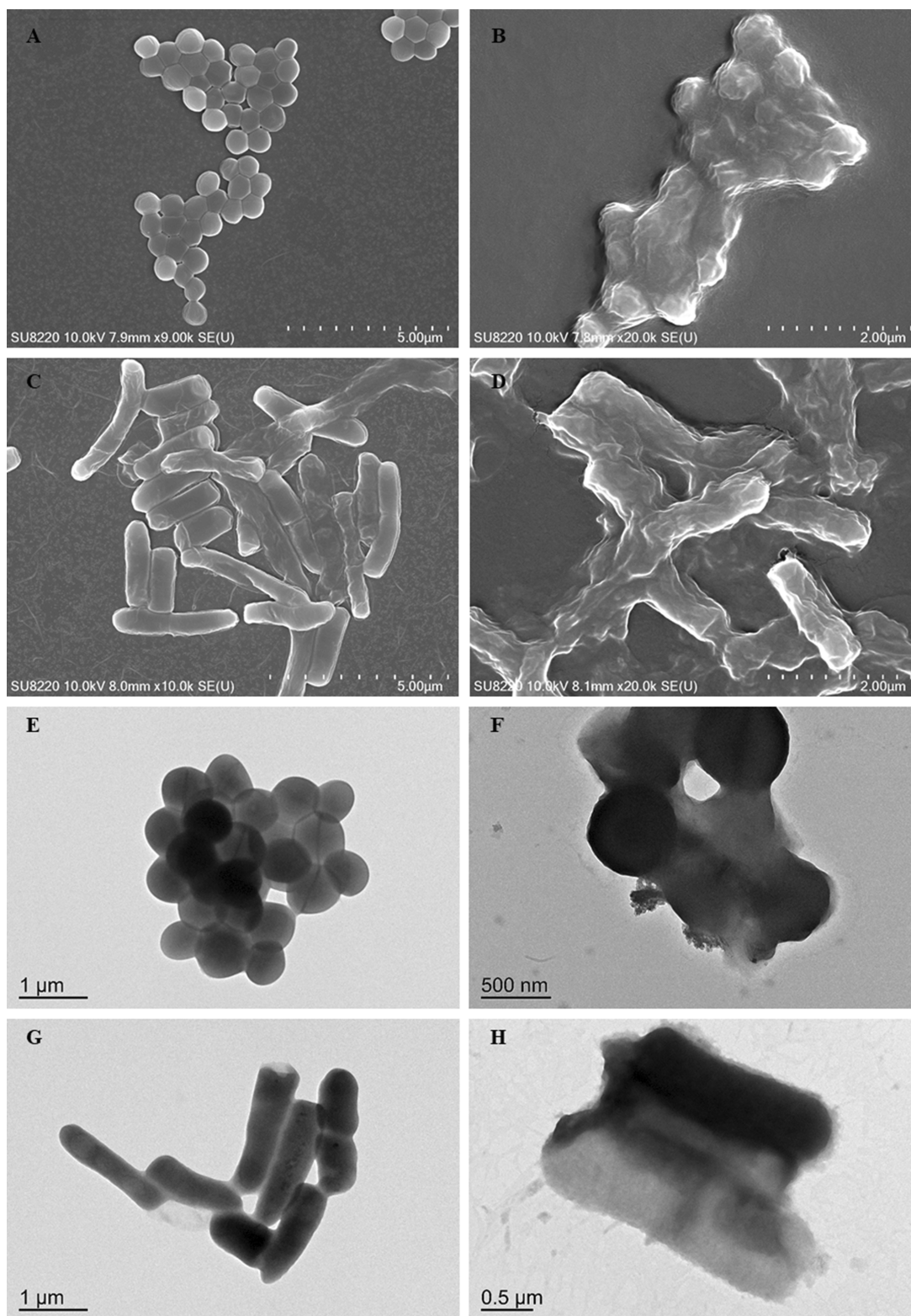


Figure 15 Morphology of the PCC liposomes-treated *S. aureus* and *E. coli* observed by SEM and TEM.

Notes: The untreated *S. aureus* (A, E) and *E. coli* (C, G), the PCC liposomes-treated *S. aureus* (B, F) and *E. coli* (D, H).

Abbreviations: PCC, photo-responsive *Camellia* sapogenin derivative cationic; SEM, scanning electron microscope; TEM, transmission electron microscope.

nm laser, which leads to bacterial lipid peroxidation, membrane permeability and oxidative damage to DNA, RNA and proteins, ultimately cell death.⁵

Conclusions

The prepared PE-MAH was grafted onto CMC by amide condensation reaction to obtain liposome shell material CMC-PE. Then, the PCC liposomes were prepared by film dispersion method using CMC-PE, soybean lecithin, cholesterol, CSD, and pheophorbide-a. The properties of PCC liposomes were characterized by size distribution, zeta potential, DL, EE, FM, SEM and TEM, confirming that pheophorbide-a is uniformly dispersed in the phospholipid bilayer and that CSD is encapsulated in liposomes. The PCC liposomes have storage stability and gastrointestinal stability. Irradiation at 665 nm stimulates pheophorbide-a to release CSD from the PCC liposomes. The PCC liposomes have strong antibacterial activity and bacterial biofilm growth inhibition, and their antibacterial activity can be significantly improved under illumination. The positive charge on surface of the PCC liposomes can produce synergistic antibacterial action with CSD and singlet oxygen to destroy the cell membrane structure of bacteria, leading to cell death. The photo-responsive PCC liposomes are efficient antibacterial agents to avoid bacterial resistance.

Acknowledgments

The authors are grateful to the staff at South China University of Technology for the data analysis they provided. Financial support from the Guangdong Natural Science Foundation Projects (Grant No. 2018B030315010) is also acknowledged.

Disclosure

The authors report no conflicts of interest in this work.

References

1. Xi YJ, Song T, Tang SY, et al. Preparation and antibacterial mechanism insight of polypeptide-based micelles with excellent antibacterial activities. *Biomacromolecules*. 2016;17(12):3922–3930. doi:10.1021/acs.biomac.6b01285
2. Cécile M, Stermitz FR, George T, et al. Isoflavones as potentiators of antibacterial activity. *J Agric Food Chem*. 2003;51(19):5677–5679. doi:10.1021/jf0302714
3. Obonyo M, Zhang L, Thamphiwatana S, et al. Antibacterial activities of liposomal linolenic acids against antibiotic-resistant *Helicobacter pylori*. *Mol Pharm*. 2012;9(9):2677–2685. doi:10.1021/mp300243w
4. Guan M, Chen YM, Wei Y, et al. Long-lasting bactericidal activity through selective physical puncture and controlled ions release of polydopamine and silver nanoparticles-loaded TiO₂ nanorods *in vitro* and *in vivo*. *Int J Nanomed*. 2019;14:2903–2914. doi:10.2147/IJN.S202625
5. Liao SJ, Zhang YP, Pan XH, et al. Antibacterial activity and mechanism of silver nanoparticles against multidrug-resistant *Pseudomonas aeruginosa*. *Int J Nanomed*. 2019;14:1469–1487. doi:10.2147/IJN.S191340
6. Araújo RD, Barbosa JM, Scotti MT, et al. Modulation of drug resistance in staphylococcus aureus with coumarin derivatives. *Scientifica*. 2016;15:1–6.
7. Tanud T, John B, Apichart S, et al. Antimycobacterial activity of cinnamate-based esters of the triterpenes botulinic, oleanolic and ursolic acids. *Chem Pharm Bull*. 2010;39(32):194–198.
8. Ye Y, Xing HT, Chen XL. Anti-inflammatory and analgesic activities of the hydrolyzed sasanqua saponins from the defatted seeds of *Camellia oleifera*. *Arch Pharm Res*. 2013;36(8):941–951. doi:10.1007/s12272-013-0138-y
9. Ye Y, Yang Q, Fang F, et al. The Camelliagenin from defatted seeds of *Camellia oleifera* as antibiotic substitute to treat chicken against infection of *Escherichia coli* and *Staphylococcus aureus*. *BMC Vet Res*. 2015;11(1):214. doi:10.1186/s12917-015-0529-z
10. Thakur M, Melzig MF, Fuchs H, et al. Chemistry and pharmacology of saponins: special focus on cytotoxic properties. *Botanics*. 2011;1:19–29.
11. Cheng SY, Wang CM, Cheng HL, et al. Biological activity of oleanane triterpene derivatives obtained by chemical derivatization. *Molecules*. 2013;18(10):13003–13019. doi:10.3390/molecules181013003
12. Keduo Q, Reen-Yun K, Chin-Ho C, et al. Anti-AIDS agents 81. Design, synthesis, and structure-activity relationship study of botulinic acid and moronic acid derivatives as potent HIV maturation inhibitors. *J Med Chem*. 2010;53(8):3133–3141. doi:10.1021/jm901782m
13. Ren TY, Lin XY, Zhang QY, et al. Encapsulation of azithromycin ion pair in liposome for enhancing ocular delivery and therapeutic efficacy on dry eye. *Mol Pharm*. 2018;15:4862–4871. doi:10.1021/acs.molpharmaceut.8b00516
14. Zhang XR, Lei B, Wang YZ, et al. Dual-sensitive on-off switch in liposome bilayer for controllable drug release. *Langmuir*. 2019;35:5213–5220. doi:10.1021/acs.langmuir.8b04094
15. Cuomo F, Mosca M, Murgia S, et al. Evidence for the role of hydrophobic forces on the interactions of nucleotide-monophosphates with cationic liposomes. *J Colloid Interface Sci*. 2013;410(22):146–151. doi:10.1016/j.jcis.2013.08.013
16. Forier K, Raemdonck K, Smedt SCD, et al. Lipid and polymer nanoparticles for drug delivery to bacterial biofilms. *J Control Release*. 2014;190:607–623. doi:10.1016/j.jconrel.2014.03.055
17. Wang H, Shi XF, Yu DF, et al. Antibacterial activity of geminized amphiphilic cationic homopolymers. *Langmuir*. 2015;31:13469–13477. doi:10.1021/acs.langmuir.5b03182
18. Lin MH, Hung CF, Aljuffali IA, et al. Cationic amphiphile in phospholipid bilayer or oil-water interface of nanocarriers affects planktonic and biofilm bacteria killing. *Nanomed Nanotechnol Biol Med*. 2016;13:353–361. doi:10.1016/j.nano.2016.08.011
19. Nitin J, Rama S, Thanigaivel S, et al. Carboxymethyl-chitosan-tethered lipid vesicles: hybrid nanoblanket for oral delivery of paclitaxel. *Biomacromolecules*. 2013;14(7):2272–2282. doi:10.1021/bm400406x
20. Hardiansyah A, Huang LY, Purwasmita BS, et al. Novel pH-sensitive drug carriers of carboxymethyl-hexanoyl chitosan (Chitosonic Acid[®]) modified liposomes. *RSC Adv*. 2015;5:23134–23143. doi:10.1039/C4RA14834G
21. Fu YY, Zhang L, Yang Y, et al. Synergistic antibacterial effect of ultrasound microbubbles combined with chitosan-modified polymyxin B-loaded liposomes on biofilm-producing *Acinetobacter baumannii*. *Int J Nanomed*. 2019;14:1805–1815. doi:10.2147/IJN.S186571
22. Lei M, Ma G, Sha S, et al. Dual-functionalized liposome by co-delivery of paclitaxel with sorafenib for synergistic antitumor efficacy and reversion of multidrug resistance. *Drug Deliv*. 2019;26:262–272. doi:10.1080/10717544.2019.1580797
23. Zhang C, Dan W, Lu L, et al. Multifunctional hybrid liposome as a theragnostic platform for magnetic resonance imaging guided photothermal therapy. *ACS Biomater Sci Eng*. 2018;4(7):2597–2605. doi:10.1021/acsbiomaterials.8b00176

24. Zhan FX, Chen W, Wang ZJ, et al. Acid-activatable prodrug nanogels for efficient intracellular doxorubicin release. *Biomacromolecules*. 2011;12(10):3612–3620. doi:10.1021/bm200876x
25. Liu CY, Jia G, Yang WL, et al. Magnetic mesoporous silica microspheres with thermo-sensitive polymer shell for controlled drug release. *J Mat Chem*. 2009;19(27):4764–4770. doi:10.1039/b902985k
26. Zhang H, Xue YN, Huang J, et al. Tailor-made magnetic nanocarriers with pH-induced charge reversal and pH-responsiveness to guide subcellular release of doxorubicin. *J Mater Sci*. 2015;50(6):2429–2442. doi:10.1007/s10853-014-8798-7
27. Alvarez-Lorenzo C, Bromberg L, Concheiro A. Light-sensitive intelligent drug delivery systems. *Photochem Photobiol*. 2010;85(4):848–860. doi:10.1111/j.1751-1097.2008.00530.x
28. Ye Y, Xing HT, Li Y. Nanoencapsulation of the sasanqua saponin from *Camellia oleifera*, its photo responsiveness and neuroprotective effects. *Int J Nanomed*. 2014;2014(1):4475–4484. doi:10.2147/IJN.S64313
29. Yang Q, Zhao C, Zhao J. Photoresponsive nanocapsulation of cobra neurotoxin and enhancement of its central analgesic effects under red light. *Int J Nanomed*. 2017;12:3463–3470. doi:10.2147/IJN.S132510
30. Qian Y. Preparation and antibacterial activity of photoresponsive *Camellia sapogenin* derivative cationic liposomes [dissertation]. Guangzhou: South China University of Technology; 2018.
31. Wu T, Zang XX, He MY, et al. Structure-activity relationship of flavonoids on their anti-*Escherichia coli* activity and inhibition of DNA gyrase. *J Agric Food Chem*. 2013;61(34):8185–8190. doi:10.1021/jf402222v
32. Lopes NA, Pinilla CM, Brandelli A. Antimicrobial activity of lysozyme-nisin co-encapsulated in liposomes coated with polysaccharides. *Food Hydrocoll*. 2019;93:1–9. doi:10.1016/j.foodhyd.2019.02.009
33. Li ZG, Chen J, Sun WQ, et al. Investigation of archaeosomes as carriers for oral delivery of peptides. *Biochem Biophys Res Commun*. 2010;394(2):412–417. doi:10.1016/j.bbrc.2017.02.010
34. Yan XM, Tang BX, Liu MF. Phenanthrenes from *Arundina graminifolia* and *in vitro* evaluation of their antibacterial and anti-haemolytic properties. *Nat Prod Res*. 2018;32(6):707–710. doi:10.1080/14786419.2017.1332606
35. Huigens RWI, Richards JJ, Parise G, et al. Inhibition of *Pseudomonas aeruginosa* biofilm formation with bromoageliferin analogues. *J Am Chem Soc*. 2007;129(22):6966–6967. doi:10.1021/ja069017t
36. H Q S, Sun FJ, Chen JH, et al. Opposite effects of cefoperazone and ceftazidime on S-ribosylhomocysteine lyase/autoinducer-2 quorum sensing and biofilm formation by an *Escherichia coli* clinical isolate. *Mol Med Rep*. 2014;10(5):2334–2340. doi:10.3892/mmr.2014.2540
37. He B, Ma S, Peng G, et al. TAT-modified self-assembled cationic peptide nanoparticles as an efficient antibacterial agent. *Nanomed-Nanotechnol*. 2018;14(2):365–372. doi:10.1016/j.nano.2017.11.002
38. Liu Q, Su RC, Yi WJ, et al. pH and reduction dual-responsive dipeptide cationic lipids with α -tocopherol hydrophobic tail for efficient gene delivery. *Eur J Med Chem*. 2017;129:1–11. doi:10.1016/j.ejmech.2017.02.010
39. Zhi DF, Zhang SB, Cui SH, et al. The headgroup evolution of cationic lipids for gene delivery. *Bioconjugate Chem*. 2013;24(4):487–519. doi:10.1021/bc300381s

International Journal of Nanomedicine

Dovepress

Publish your work in this journal

The International Journal of Nanomedicine is an international, peer-reviewed journal focusing on the application of nanotechnology in diagnostics, therapeutics, and drug delivery systems throughout the biomedical field. This journal is indexed on PubMed Central, MedLine, CAS, SciSearch®, Current Contents®/Clinical Medicine,

Journal Citation Reports/Science Edition, EMBase, Scopus and the Elsevier Bibliographic databases. The manuscript management system is completely online and includes a very quick and fair peer-review system, which is all easy to use. Visit <http://www.dovepress.com/testimonials.php> to read real quotes from published authors.

Submit your manuscript here: <https://www.dovepress.com/international-journal-of-nanomedicine-journal>